



**Tailoring Electron Transfer Pathway for Photocatalytic N<sub>2</sub>-  
to-NH<sub>3</sub> Reduction in a CdS Quantum Dots-Nitrogenase  
System**

Journal:	<i>Sustainable Energy &amp; Fuels</i>
Manuscript ID	SE-ART-01-2022-000148.R1
Article Type:	Paper
Date Submitted by the Author:	16-Mar-2022
Complete List of Authors:	Badalyan, Artavazd; Utah State University, Chemistry and Biochemistry Yang, Zhi-Yong; Utah State University, Chemistry and Biochemistry Hu, Maowei; Utah State University, chemistry and biochemistry Liu, Tianbiao; Utah State University, Chemistry and Biochemistry Seefeldt, Lance; Utah State University, Chemistry and Biochemistry

## Tailoring Electron Transfer Pathway for Photocatalytic N<sub>2</sub>-to-NH<sub>3</sub> Reduction in a CdS Quantum Dots-Nitrogenase System

Artavazd Badalyan,<sup>\*a</sup> Zhi-Yong Yang,<sup>a</sup> Maowei Hu,<sup>a</sup> T. Leo Liu,<sup>a</sup> Lance C. Seefeldt<sup>\*a</sup>

Received 00th January 20xx,  
Accepted 00th January 20xx

DOI: 10.1039/x0xx00000x

The combination of abiotic photosensitizers with purified enzymes in a biohybrid system offers a promising pathway to utilizing light to accomplish challenging chemical transformations and provides insights into the rational photocatalytic system design for efficient solar-to-chemical energy conversion. In this work, we demonstrate a hybrid photocatalytic system for ammonia production from N<sub>2</sub> by combining cadmium sulfide quantum dots (CdS QDs) and Mo-nitrogenase from *Azotobacter vinelandii*, composed of the iron protein (FeP) and the molybdenum-iron protein (MoFeP). Photoexcited electrons from the CdS QD are delivered by an electron transfer mediator through the FeP to the catalytic MoFeP. The complete system was optimized for the ligand on the CdS QDs, mediators, and reaction conditions. The best results were achieved with β-mercaptoethanol as a QD ligand. The mediator test revealed that 1,1'-bis(3-sulfonatopropyl)-4,4'-bipyridinium (SPR)<sub>2</sub>V (-0.4 V vs. NHE) supports the reduction of protons and N<sub>2</sub> to H<sub>2</sub> and ammonia catalyzed by nitrogenase. However, in the presence of 1,1'-trimethylene-2,2'-bipyridinium TQ (-0.58 V vs. NHE) as a mediator, nitrogenase catalysis resulted in remarkably more products. The UV-vis and *in-situ* potentiometric studies revealed that better performance with TQ is achieved due to the significantly more negative solution potential allowing for efficient reduction of FeP. As a result, the quantum yield for conversion of absorbed photons to ammonia attains 16%, far exceeding that of previously reported nitrogenase-based systems. This work reveals the importance of tuning the electron transfer pathways in photocatalytic systems and illustrates a potent strategy for efficient electronic coupling of a photosensitizer and an N<sub>2</sub> reduction catalyst.~

### Introduction

The selective reduction of N<sub>2</sub> to ammonia is vital for life.<sup>1</sup> The industrial production of ammonia occurs primarily through the energy-intensive and environmentally burdensome Haber-Bosch process.<sup>2</sup> Significant efforts have been focused on the development of catalysts that can reduce N<sub>2</sub> (using protons and electrons) under mild conditions.<sup>3–8</sup> The utilization of renewable and abundant solar energy to drive catalytic N<sub>2</sub> reduction is a promising way not only for “green” ammonia synthesis, but also for decentralization of ammonia production<sup>9,10</sup> and the use of ammonia for energy storage.<sup>11–13</sup> Photodriven ammonia production will require efficient coupling of a photosensitizer and the nitrogen reduction catalyst.

Quantum dots (QDs) and related nanostructures are ideal photosensitizers for light harvesting and charge separation applications because they offer tunable bandgaps, absolute redox potentials, and various chemical functional groups ideal for optimizing to specific targets and reaction environments.<sup>14,15</sup> A strategy for coupling light-driven electron transfer from QD to achieve N<sub>2</sub> reduction is illustrated in Figure 1. In this strategy, photochemical N<sub>2</sub> reduction starts with the light absorption and the charge separation at QDs followed by the electron transfer from QDs to the catalyst directly or using

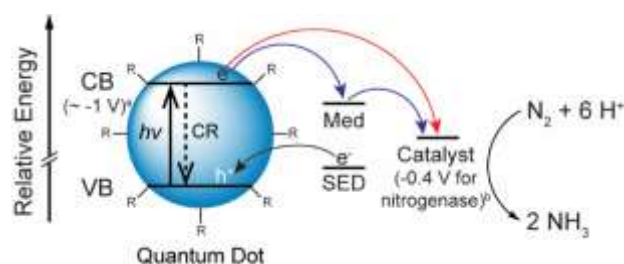


**Figure 1.** Schematic depiction of relevant processes in a photocatalytic N<sub>2</sub> to ammonia reduction by a QD, or related nanostructure, and N<sub>2</sub> reduction catalyst utilizing direct (red) and mediated (blue) electron transfer. CB and VB are conduction and valence bands of a nanostructure, R is the functional group of a ligand coordinated to the CdS nanostructure, CR is charge recombination, Med is electron transfer mediator, SED is a sacrificial electron donor. a, Potentials are given versus NHE. b, Formal potential of [4Fe4S]-cluster of nitrogenase FeP measured at pH 8.

Electron transfer mediators, followed by the reduction of N<sub>2</sub> (Figure 1). The overall photocatalytic efficiency, i.e., quantum yield for the conversion of absorbed photons to ammonia, is determined by the efficiencies of involved processes, which can be improved by the advancement of N<sub>2</sub> reduction catalysts and approaches for charge separation and light-harvesting.

The combination of a QD with an enzyme as a model catalyst results in a biohybrid that integrates an efficient transformation of absorbed photon energy into redox equivalents and outstanding catalytic properties of redox enzymes for solar-to-chemical energy conversion.<sup>16</sup> Biohybrids as proof-of-principle photocatalytic systems provide insights into the optimal design and efficiencies of photocatalytic approaches. For this, enzymes are isolated from their biological environment and coupled with QD directly<sup>16–24</sup> or using electron transfer mediators.<sup>25–28</sup> Being the only N<sub>2</sub> reducing enzyme in nature, nitrogenase is of

<sup>a</sup> Department of Chemistry and Biochemistry, Utah State University, 0300 Old Main Hill, Logan, UT 84322, USA.

\*Corresponding authors: [a.badalyan@usu.edu](mailto:a.badalyan@usu.edu) and [lance.seefeldt@usu.edu](mailto:lance.seefeldt@usu.edu).

Electronic Supplementary Information (ESI) available: Photoreduction of (SPR)<sub>2</sub>V by CdS QDs-ME, the CdS QDs ligand test, CdS QDs-ME and ME effects on nitrogenase activity, UV-vis studies of (SPR)<sub>2</sub>V and TQ photochemical reduction, estimation of quantum yields. See DOI: 10.1039/x0xx00000x

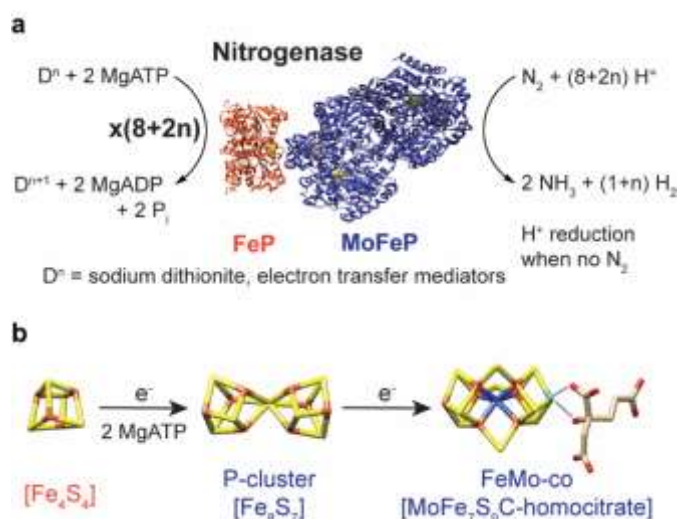
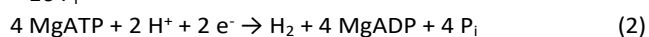
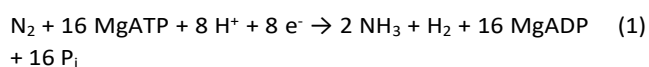


**Figure 2.** (a) Simplified catalytic scheme of *in vitro* nitrogenase catalysis. (b) Electron transfer between redox cofactors of nitrogenase. Shown is Fe in orange, S in yellow, C in blue, Mo in cyan, and O in red.

particular interest for the development of a biohybrid because it is capable of the crucial multi-electron N<sub>2</sub> to ammonia reduction with high catalytic rate and selectivity under ambient conditions (Figure 2).

The molybdenum-dependent nitrogenase consists of two component proteins (Figure 2a) called the iron protein (FeP) and the molybdenum-iron protein (MoFeP).<sup>29</sup> FeP houses a single [4Fe-4S] cluster and two MgATP binding sites.<sup>30</sup> MoFeP contains two unique cofactors, the electron carrier [8Fe-7S] (P-cluster) and the catalytic [7Fe-9S-1Mo-C-homocitrate] (FeMo-co).<sup>31,32</sup> During the catalytic cycle, FeP binds two MgATP molecules and is reduced either by flavodoxin or ferredoxin (*in vivo*)<sup>33,34</sup> or sodium dithionite or electron transfer mediators (*in vitro*)<sup>35–38</sup>. The FeP then transiently associates with the MoFeP,<sup>39</sup> transfers a single electron to the P-cluster of MoFeP, which ultimately accumulates on the FeMo-co (Figure 2b). The two MgATP molecules are then hydrolyzed, triggering the oxidized FeP (with two bound MgADP) to dissociate from the one-electron reduced MoFeP. The released FeP is reduced again, and the two MgADP molecules are replaced by two MgATP, to prepare the system for another round of association, electron transfer, ATP hydrolysis, and dissociation. This cycle is called the FeP cycle and is repeated 8 times delivering 8 electrons and 8 protons to the FeMo-co catalytic site to reduce an N<sub>2</sub> to two ammonia molecules coupled with the production of one H<sub>2</sub> (eq 1).<sup>40,41</sup> This ratio of products is observed under high N<sub>2</sub> pressure (50 atm) and the maximal catalytic rate (Figure 2a, n=0).<sup>42</sup> Under 1 atm N<sub>2</sub> and conditions corresponding to slower enzymatic reaction rates, more H<sub>2</sub> per ammonia is produced (Figure 2a, n>0). In the absence of N<sub>2</sub>, nitrogenases catalyze the reduction of protons (eq 2).



In this work, we demonstrate a biohybrid system for ammonia production combining CdS QD, nitrogenase, and an electron transfer mediator. The catalytic performance of the biohybrid system was studied with respect to the functional groups of the quantum dots, electron transfer mediators, and reaction conditions under argon and N<sub>2</sub>.

## Results and Discussion

**Characterization of CdS QDs and photochemical reduction of the mediator (SPr)<sub>2</sub>V.** CdS QDs bearing β-mercaptoethanol (ME) as a ligand (CdS QDs-ME) were synthesized (see Experimental section for more information). The first exciton absorption peak is at 420 nm corresponding to an estimated diameter of 4.1 nm (Figure 3a).<sup>43</sup> The concentration was estimated as described elsewhere.<sup>43</sup> (SPr)<sub>2</sub>V was chosen as a mediator because its one-electron reduced radical form [(SPr)<sub>2</sub>V<sup>•-</sup>] was previously determined as an efficient electron donor to FeP in support of substrate reduction.<sup>38</sup> The photochemical reduction of (SPr)<sub>2</sub>V was performed in the presence of 100 nM CdS QDs-ME and 2 mM ME in nitrogenase activity buffer containing 100 mM 3-morpholinopropane-1-sulfonic acid (MOPS), pH 7.0, 6.7 mM MgCl<sub>2</sub>, 5 mM ATP, and an ATP regeneration system (30 mM phosphocreatine and 0.2 mg/ml kinase), at room temperature (Figure 3b). MOPS acted as a sacrificial electron donor (SED).<sup>44</sup> The illumination of this mixture using 405 nm light-emitting diode (93 μmol photons m<sup>-2</sup> s<sup>-1</sup>) led to a reduction of (SPr)<sub>2</sub>V to [(SPr)<sub>2</sub>V<sup>•-</sup>] (Figure 3b). The ten minutes reaction time was chosen as optimal to study and find an optimal electron transfer pathway in the proposed system. No heating of a sample was observed after 10 minutes of irradiation. The formation of [(SPr)<sub>2</sub>V<sup>•-</sup>] was followed spectrophotometrically at wavelength 600 nm. The system was studied with respect to (SPr)<sub>2</sub>V concentration and showed a saturating behavior (Figures 3c, S1). Varying the concentration of CdS QDs-ME in the presence of 2 mM (SPr)<sub>2</sub>V resulted in a linear trend up to 200 nM CdS QDs-ME (Figures 3d, S2). The effects of ME concentration and photon flux were also studied. The addition of higher concentrations of ME was not beneficial for the mediator reduction (Figure S3a). The increase of the photon flux resulted in higher amounts of the reduced mediator (Figure S3b).

After confirming that CdS QDs-ME photochemically reduce the electron transfer mediator (SPr)<sub>2</sub>V, the effect of ligands of CdS QDs on the (SPr)<sub>2</sub>V reduction was studied (Figure S4). QDs bearing carboxylic and amino groups showed significant amounts of the reduced mediator. However, CdS QDs decorated with hydroxyl groups were particularly effective in nitrogenase activity buffer and were used for further studies.

To examine the effect of CdS QDs-ME on nitrogenase activity, standard spectrophotometric activity assays were performed varying CdS QDs-ME concentrations. This study revealed no inhibitory effects of CdS QDs-ME on nitrogenase activity (Figure S5a). ME concentrations of up to 40 mM also did not affect nitrogenase activity (Figure S5b and c). Thus, 100 nM CdS QDs-ME, 2 mM ME, and the photon flux of 93 μmol m<sup>-2</sup> s<sup>-1</sup> were chosen for further studies.

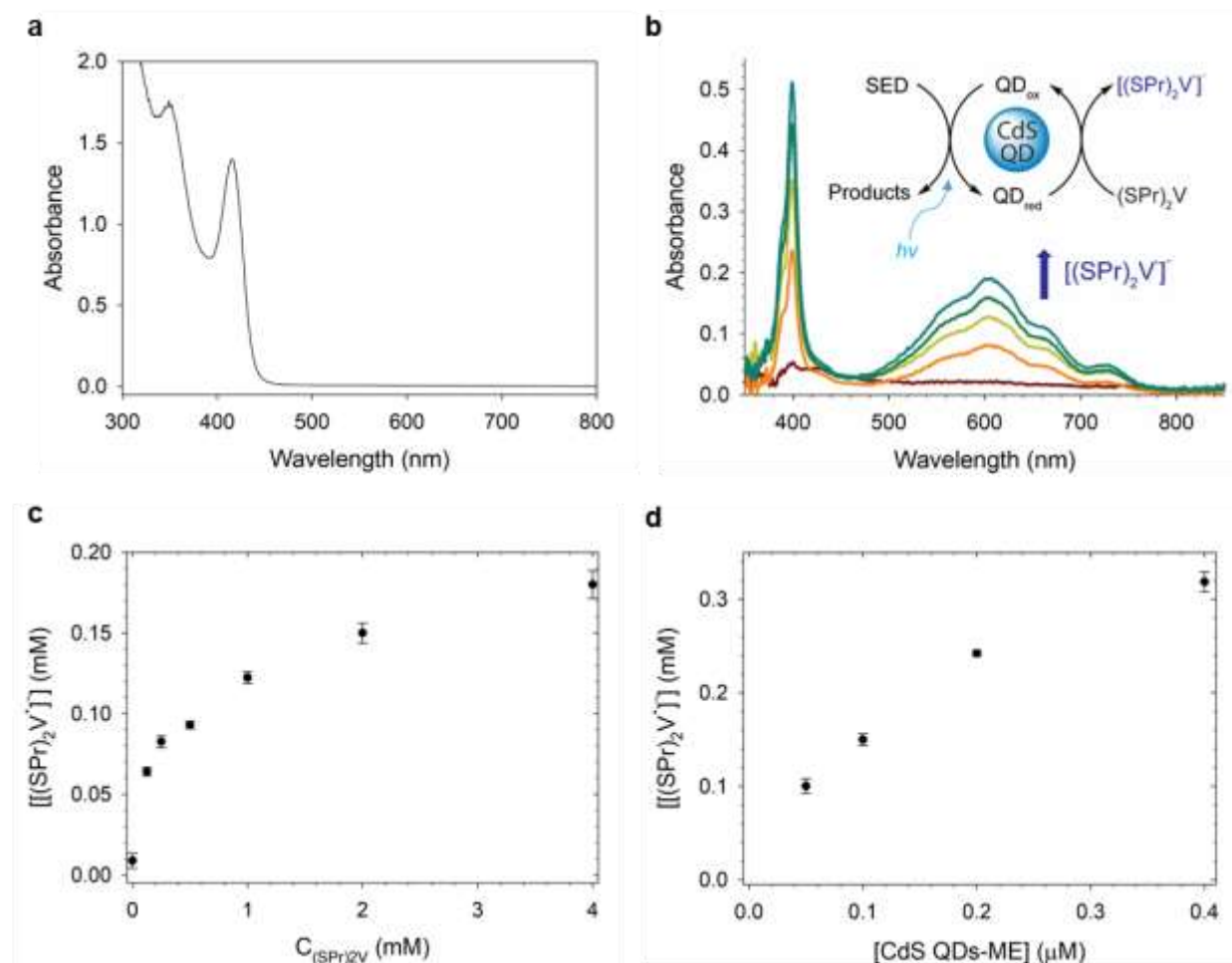


**Figure 3. Photoreduction of  $(\text{SPr})_2\text{V}$  by CdS QDs-ME.** a, The UV-vis spectrum of CdS QDs-ME in 10 mM KCl, cuvette pathlength is 10 mm. b, The spectrophotometric evidence of the photoreduction of  $(\text{SPr})_2\text{V}$  by CdS QDs-ME and a simplified scheme of this process. Conditions: 2 mM  $(\text{SPr})_2\text{V}$ , 100 nM CdS QDs-ME, cuvette pathlength is 2 mm. The spectra correspond to 0, 2.5, 5, 7.5, 10 min illumination. c, Plot of  $[(\text{SPr})_2\text{V}]$  versus  $[(\text{SPr})_2\text{V}]$  in the presence of 100 nM CdS QDs-ME. d, Plot  $[(\text{SPr})_2\text{V}]$  versus  $[\text{CdS QDs-ME}]$  in the presence of 2 mM  $(\text{SPr})_2\text{V}$ . All experiments were performed in the nitrogenase activity buffer with 2 mM ME, excitation wavelength 405 nm, 10 minutes, 0.5 ml,  $n=3$ .

**Nitrogenase photocatalysis under argon.** MoFeP and FeP were added to a sealed vial containing nitrogenase activity buffer, 0.1  $\mu\text{M}$  CdS QDs-ME, and 2 mM  $(\text{SPr})_2\text{V}$  (Figure 4a). The reaction solution was exposed to the light, and the formed  $\text{H}_2$  was determined by gas chromatography. The time course of this reaction showed a linear trend for  $\text{H}_2$  formed versus time in up to ten minutes experiment (Figure 4b). When the mixture was not illuminated or CdS QDs-ME, FeP, MoFeP, FeP-MoFeP, or ATP regeneration system were absent, negligible or no  $\text{H}_2$  was detected.

**Electron transfer mediators.** To find an optimal electron transfer mediator, a solution containing 2 mM of one of six different mediators (Figures 4c and d), CdS QDs-ME, MoFeP, FeP in nitrogenase activity buffer was illuminated for 10 minutes under argon, and the produced  $\text{H}_2$  was measured. The results are summarized in Figure 4d. In the presence of diquat (DQ) and benzyl viologen ( $\text{Bz}_2\text{V}$ ), only a negligible amount of  $\text{H}_2$  was formed. Similar amounts of  $\text{H}_2$  were formed with  $(\text{SPr})_2\text{V}$  (-0.40 V vs. NHE), methyl viologen ( $\text{Me}_2\text{V}$ , -0.44 V vs. NHE), and ethyl viologen ( $\text{Et}_2\text{V}$ , -0.45 V vs. NHE). A much higher amount of  $\text{H}_2$

was observed with the lowest potential mediator used in this study, triquat (TQ, -0.58 V vs. NHE). The control experiments were performed for TQ-mediated system and revealed that in the absence of FeP, MoFeP, or ATP and ATP regeneration system, negligible amounts of  $\text{H}_2$  were formed, indicating that observed  $\text{H}_2$  is a product of TQ-mediated nitrogenase catalysis. The mediator's performance in this test is a sum of two processes, photochemical reduction of the mediator and electron transfer from the reduced mediator to nitrogenase. The UV-vis studies of the CdS QDs-ME/TQ and CdS QDs-ME/ $(\text{SPr})_2\text{V}$  after 10 min illumination did not reveal significant differences in the amounts of the reduced forms of the mediators (Figure S6). This indicates that the electron transfer between the mediator and nitrogenase, i.e.,  $[\text{4Fe4S}]$  cluster of FeP, plays a crucial role in the observed differences of the performance of the mediators. In the presence of nitrogenase, no characteristic colors associated with the reduced form of mediators were observed due to fast consumption of reduced form of mediators by nitrogenase.

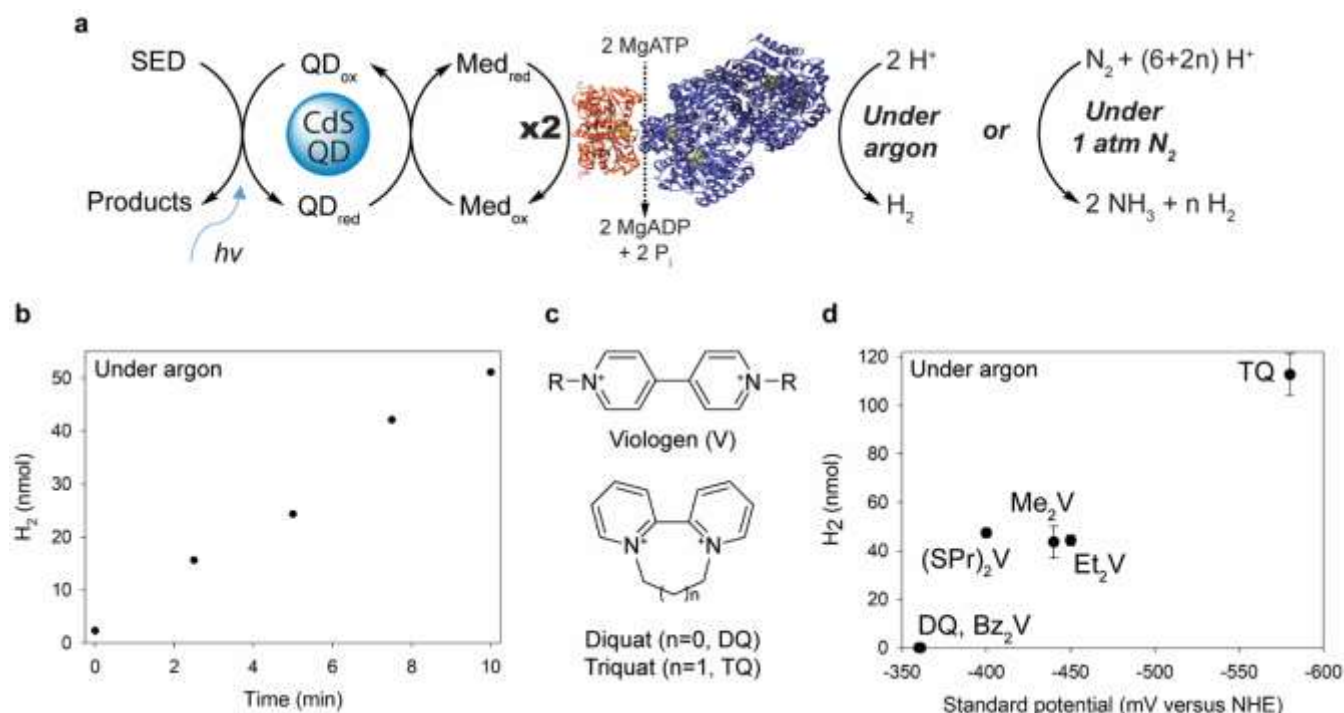


**Figure 4. Nitrogenase photocatalysis under argon and mediator performance.** a, A simplified scheme of nitrogenase photocatalysis. b, The time course of  $H_2$  formation with  $(SPr)_2V$  as a mediator ( $n=1$ ). c, Chemical structures of mediators. d, The amount of  $H_2$  formed versus the standard potential of mediators under argon ( $n=3$ ). Bz is benzyl, Me is methyl, Et is ethyl. Conditions:  $0.1 \mu M$  CdS QDs-ME,  $2 \text{ mM}$  mediator,  $0.4 \mu M$  MoFeP,  $6 \mu M$  FeP,  $2 \text{ mM}$  ME in nitrogenase activity buffer, excitation wavelength  $405 \text{ nm}$ , illumination time  $10 \text{ min}$ ,  $0.5 \text{ mL}$ .

**Electrochemical solution potential.** The *in-situ* potentiometric studies were performed in nitrogenase activity buffer containing  $0.1 \mu M$  CdS QDs-ME and  $2 \text{ mM}$  of the corresponding mediator in the absence of nitrogenase. The ten minutes long illumination of the solution started after the second minute of an experiment (Figure 5). For both  $(SPr)_2V$  and TQ, the potential reached a plateau after approximately 80 seconds. However, the plateau potentials were significantly different,  $(SPr)_2V - -320 \text{ mV}$  and TQ  $- -460 \text{ mV}$  (vs. NHE).

The  $(SPr)_2V$  plateau potential was slightly more negative than the formal potential of the  $[4Fe4S]$  cluster of FeP with no bound nucleotides ( $-0.29 \text{ V}$  vs. NHE) but significantly higher than that for FeP in the presence of bound MgATP or MgADP ( $-0.43 \text{ V}$  and  $-0.44 \text{ V}$  vs. NHE, measured at pH 8).<sup>45,46</sup> This indicates that the electron transfer from the reduced mediator to a free FeP can occur, whereas, in the presence of nucleotides, the electron transfer is thermodynamically disfavored. On the other hand, the plateau potential generated by the CdS QDs-ME/TQ system was more negative than the potentials of free and nucleotide-bound FeP, indicating that electron transfer to all forms of FeP is favorable.

To estimate the population of reduced FeP under conditions used in this study, the following two assumptions were made. First, the reduction of FeP-2MgATP does not affect redox equilibrium controlled by the mediator redox couple ( $[FeP] \ll [Med_{red}]$ ). Second, all FeP is in the FeP-2MgATP form due to the high concentration of MgATP. The Nernst equation (eq 3) can be transformed to equation 4 where  $E$  is the solution plateau potential,  $E^{\circ'}$  is the formal potential of FeP-2MgATP

redox couple. Thus, the reduced FeP-2MgATP was calculated to be  $\sim 1.4\%$  in the  $(SPr)_2V$  solution and  $69\%$  in the TQ solution. Though these calculations reflect only the thermodynamics of electron transfer from a reduced mediator to the FeP-2MgATP, this estimation points to the significant role of the solution potential. It also shows a rationale to tailor the solution potential using appropriate electron transfer mediators to obtain an efficient photocatalytic system.

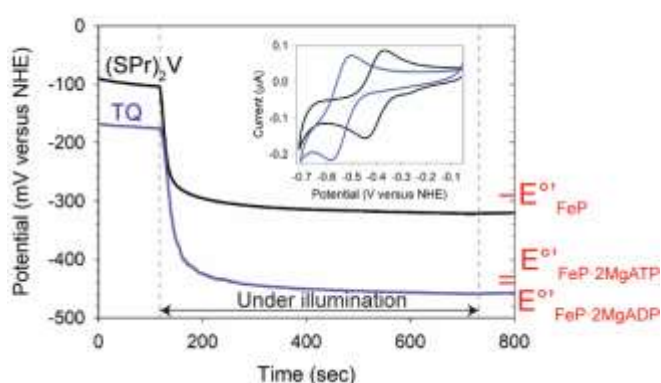


**Figure 5. *In-situ* potentiometry of CdS QDs-ME/ $(SPr)_2V$  and CdS QDs-ME/TQ systems under argon.** Conditions:  $0.1 \mu M$  CdS QDs-ME,  $2 \text{ mM}$  mediator,  $2 \text{ mM}$  ME in nitrogenase activity buffer, excitation wavelength  $405 \text{ nm}$ , illumination time  $10 \text{ min}$ ,  $0.5 \text{ mL}$ . Inset, cyclic voltammograms of  $50 \mu M$   $(SPr)_2V$  (in black) and TQ (in blue) recorded in nitrogenase activity assay buffer,  $5 \text{ mV s}^{-1}$ .

$$E = E^{o'} + 0.059 \log_{10} \left( \frac{[FePOx \cdot 2MgATP]}{[FeP_{Red} \cdot 2MgATP]} \right) \rightarrow \frac{[FePOx \cdot 2MgATP]}{[FeP_{Red} \cdot 2MgATP]} = 10^{\frac{E - E^{o'}}{0.059}} \quad (3)$$

$$\frac{[FeP_{Red} \cdot 2MgATP]}{[FeP \cdot 2MgATP]_{total}} = \frac{1}{1 + 10^{\frac{E - E^{o'}}{0.059}}} \quad (4)$$

**(SPr)<sub>2</sub>V versus TQ under 1 atm N<sub>2</sub>.** The performances of (SPr)<sub>2</sub>V and TQ were also studied under 1 atm N<sub>2</sub>, and H<sub>2</sub> and ammonia were detected using gas chromatography and a fluorimetric assay, respectively (Figure 6a). The amount of H<sub>2</sub> formed under N<sub>2</sub> was lower than that under argon for both mediators. This is a well-known trend for nitrogenase since electrons delivered to an enzyme under N<sub>2</sub> are used to produce ammonia. Amounts of products formed in the presence of TQ were significantly higher than in the presence of (SPr)<sub>2</sub>V, indicating that TQ is a more efficient mediator for photocatalytic reduction of nitrogenase both under argon and N<sub>2</sub>.

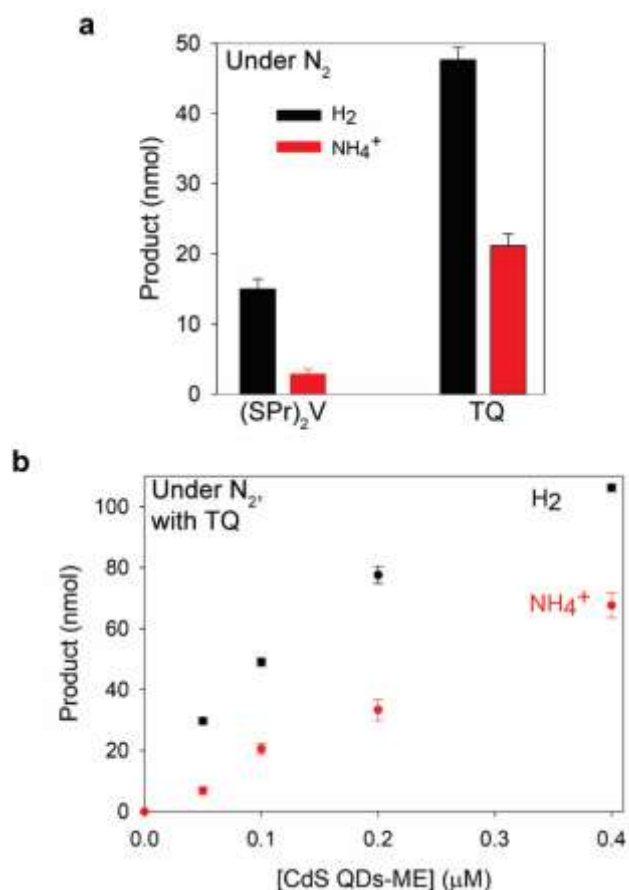


**Figure 6.** CdS QDs-ME/Mediator/nitrogenase biohybrid under 1 atm N<sub>2</sub>. **a**, Amounts of H<sub>2</sub> and NH<sub>4</sub><sup>+</sup> formed under N<sub>2</sub> using 2 mM (SPr)<sub>2</sub>V and TQ. **b**, Ammonia (red) and H<sub>2</sub> (black) formed versus [CdS QDs-ME]. Conditions: 0.1 μM CdS QDs-ME, 2 mM TQ, 0.4 μM MoFeP, 6 μM FeP, 2 mM ME in nitrogenase activity buffer under 1 atm N<sub>2</sub>, excitation wavelength 405 nm, illumination time 10 min, n=3, 0.5 mL.

**CdS QDs-ME/TQ/Nitrogenase biohybrid.** N<sub>2</sub> and H<sup>+</sup> reduction was studied as a function of [CdS QDs-ME] (Figure 6b). The amounts of products increased with the concentration of CdS QDs-ME. At 0.4 μM CdS QDs-ME, 106 nmol H<sub>2</sub> and 68 nmol NH<sub>4</sub><sup>+</sup> were formed. The quantum yields (QYs) for conversion of

absorbed photons to ammonia and both to ammonia and H<sub>2</sub> were estimated to be 16 % and 33 %, respectively (see Supporting information for more details). Important to note that the QY of the current system can be further improved by increasing the concentrations of CdS QDs and a mediator.

Based on the measured products, a turnover frequency (TOF) for nitrogenase (in mol electrons in H<sub>2</sub> and NH<sub>4</sub><sup>+</sup>/(mol MoFeP s<sup>-1</sup>)) was calculated to be 3.5 s<sup>-1</sup>. With the maximal *k*<sub>obs</sub> of ~15 s<sup>-1</sup> determined using spectrophotometric assay (see Figure S5a), the TOF corresponds to ~23 % of the maximal activity of nitrogenase. TOF can be further increased by increasing the concentration of quantum dots and photon flux.

**N<sub>2</sub> to ammonia reduction by the previously reported nitrogenase-based photocatalytic systems.** Alternative systems were reported that utilized photosensitizer and nitrogenase to reduce N<sub>2</sub>. One earlier report<sup>47</sup> uses a rather complicated system with eosin as a photosensitizer, NADH as an electron donor, and both FeP and MoFeP. Though ammonia formation was observed, the reaction stopped after 40-50 seconds presumably because eosin inhibits the FeP activity. N<sub>2</sub> to ammonia reduction was also reported for systems utilizing quantum dots and nanorods as photosensitizers and circumventing the FeP cycle, such as, CdS QDs-ME/Methyl viologen/MoFeP<sup>48</sup>, CdS nanorods<sup>49</sup> and QDs<sup>50</sup> directly coupled to MoFeP. The direct systems revealed QYs 3.3 % for nanorods<sup>49</sup> and 1.2 % for quantum dots<sup>50</sup> utilizing mercaptopropionic acid as a ligand and required much longer irradiation time and often higher energy light sources and higher temperatures to obtain significant amounts of ammonia.

The described nitrogenase biohybrid has several advantages. First, the current system shows no inhibitory effect of the photosensitizer with nitrogenase. Second, the utilization of both a mediator and FeP allowed QY to exceed that of other nitrogenase-based systems. As a result, the current system requires a short illumination time and a lower energy light source to achieve significant amounts of ammonia produced. Third, the reported system is well suited for transient spectroscopic studies of nitrogenase featuring FeP and MoFeP. Moreover, in contrast to other systems, this biohybrid can vary the reducing power in a broad potential range by changing mediators allowing to access different redox states of [4Fe4S]-cluster of FeP.

## Conclusions

This work demonstrates a biohybrid system utilizing CdS QDs and the enzyme nitrogenase that achieves photocatalytic N<sub>2</sub> reduction to ammonia. An electron transfer mediator was used as an electron shuttle that accepts and effectively accumulates electrons from the photoexcited states of CdS QDs and delivers the electrons through the FeP to the catalytic MoFeP to support the reduction of N<sub>2</sub> and protons to ammonia and H<sub>2</sub>. Importantly, no nitrogenase catalysis was observed in the absence of FeP or a mediator, indicating no alternative pathways. This outcome is most likely due to the low electron transfer efficiency from short-living excited states of QDs directly to FeP or MoFeP, resulting in the non-productive,

charge recombination processes. The current work shows that in photocatalytic experiments, the solution potential plays a crucial role in driving the catalyst nitrogenase, and can be regulated by using an appropriate mediator. Due to the highly reducing nature of the conduction band electron (about -1 V vs. NHE) of CdS QDs, the potential window between this band potential and the potential of the nitrogen reduction catalyst (in this work, [4Fe-4S] cluster of nitrogenase FeP) for choosing a mediator is broad. Harvesting more energy for QDs by using a more negative potential mediator, such as TQ, results in a more negative solution potential and supports an efficient N<sub>2</sub> to ammonia conversion with QY of 16%, far exceeding earlier QYs reported for alternative nitrogenase-based photocatalytic systems. This work indicates the importance of tuning the electron transfer pathways in photocatalytic systems and illustrates the concept of using electron transfer mediators for the efficient coupling of a photosensitizer and a catalyst for direct solar ammonia production.

## Material and methods

**Reagents and apparatus.** All commercial reagents were obtained from Sigma-Aldrich and used as received unless otherwise noted. Dihydrogen, argon, and dinitrogen were purchased from Air Liquide America Specialty Gases LLC (Plumsteadville, PA). The argon and dinitrogen gases were passed through an activated copper catalyst to remove dioxygen contamination prior to use. *A. vinelandii* strains DJ995 (wild-type MoFeP protein, UniProtKB P07328, P07329) and DJ884 (wild-type FeP, UniProtKB P00459) were grown, and nitrogenase proteins were expressed and purified as previously described.<sup>51</sup> Proteins and buffers were handled anaerobically in septum-sealed serum vials under an inert atmosphere (argon or dinitrogen), on a Schlenk vacuum line or in anaerobic glove boxes. The transfer of gases and liquids was done with gas-tight syringes.

**Synthesis of electron transfer mediators.** The synthesis of 1,1'-bis[3-sulfonatopropyl]-4,4'-bipyridinium ((SPr)<sub>2</sub>V) was described elsewhere.<sup>52</sup>

**Synthesis of CdS QDs-Oleic acid.** CdS QDs capped with oleic acid (CdS QDs-OA) were prepared using a described procedure<sup>14</sup> with some modifications. A mixture of CdO (0.0128 g, 0.1 mmol), oleic acid (634  $\mu$ L), and technological grade octadecene (2900  $\mu$ L) in a three-neck flask was heated to 300 °C under argon using a sand bath to get a clear solution. Then the mixture was cooled down to 250 °C, and a solution of sulfur (1.6 mg) in 0.5 ml octadecene was added to the flask. After 20 seconds, the flask was rapidly cooled down to room temperature (23 °C). Then the solution was transferred to a round bottom flask, mixed with 8 mL methanol and 1 mL butanol, and shaken vigorously. The mixture was centrifuged at 3500 rpm for 5 minutes. The solvent phase was removed. Then, 2 mL hexane was added, followed by an excess of acetone for precipitation. Then the mixture was centrifuged and decanted. The pellet was resuspended in chloroform, and the UV/vis spectrum was measured.

**Ligand exchange.** 86 mM 2-mercaptoethanol solution in 10 mM KCl was prepared and adjusted to pH 7.6. 4 mL of this solution was added to 2 mL CdS QDs-OA dissolved in chloroform and adjusted to an absorbance of 1 A.U. at 420 nm (cuvette pathlength 1 cm). The mixture was stirred for two hours under dark, then left for 30 minutes without stirring. The aqueous phase was transferred to another flask, diluted with 10 mM KCl aqueous solution, and centrifuged in Amicon filter units (30 k, 0.5 mL) to remove the excess ligand and to concentrate the nanocrystal solution. The final solution was studied using UV-vis spectroscopy.

**Photochemical experiments.** The photochemical experiments were performed in the glove box (MO-M, Vacuum Atmosphere Co., Hawthorne, CA) filled with argon at room temperature (23 °C). The solutions (0.5 ml) were stirred under illumination with a 405 nm diode connected to the LED controller (LDC-1, Ocean Optics) in sealed vials with a total volume of 2 mL. The amount of H<sub>2</sub> produced was determined by gas chromatography.<sup>53</sup> The amount of ammonia was determined using a fluorimetric protocol with some modifications.<sup>54</sup> A 25  $\mu$ L aliquot of a post-reaction solution was added to 1 mL of a detection solution containing 20 mM phthalic dicarboxyaldehyde, 3.5 mM 2-mercaptoethanol, 5% (v/v) ethanol, and 200 mM potassium phosphate, pH 7.3, and allowed to react in the dark for 30 min. After this, the fluorescence signal was measured using  $\lambda$  excitation of 410 nm and  $\lambda$  emission of 472 nm. An NH<sub>4</sub><sup>+</sup> standard curve was generated using NH<sub>4</sub>Cl. To account for the background signal of the photochemical reaction solutions, the control experiments were performed under 1 atm N<sub>2</sub> without illumination and under 1 atm argon with and without illumination with all corresponding additives. The background signals were relatively small and similar for all control experiments and were subtracted from the signals obtained under 1 atm N<sub>2</sub> exposed to the light.

**Potentiometry.** The solution potential was assessed by immersing two electrodes (Pt wire (0.5 mm, ALS, Japan)) as a sensing electrode and Ag|AgCl electrode as a reference electrode) in a vial and measuring the potential difference as a function of time using a potentiostat CH Instrument Model 620E (Austin, USA). The solution potential versus NHE was calculated with respect to the potential of the reference electrode. To determine the reference electrode potential, cyclic voltammograms of a reference redox compound with a known standard redox potential were recorded using the same reference electrode, a glassy carbon working electrode (diameter 3 mm, ALS, Japan) and a Pt wire counter electrode, before and after potentiometric experiments.

## Author Contributions

AB conceived the idea of the project, designed the study, and performed all experiments. AB led the data interpretation and analysis in consultation with LCS. AB synthesized CdS QDs. MH synthesized (SPr)<sub>2</sub>V under the supervision of TLL. ZY isolated

and purified MoFeP. ZY and AB isolated and purified FeP. AB and LCS wrote the manuscript.

### Conflicts of interest

There are no conflicts to declare.

### Acknowledgements

Funding was provided by the U.S. Department of Energy Office of Basic Energy Sciences, Division of Chemical Sciences, Geosciences, and Biosciences, Physical Biosciences and Solar Photochemistry Programs. M. H. and T. L. L. acknowledge the National Science Foundation (Career Award, Grant No. 1847674) for supporting the synthesis of (SPr)<sub>2</sub>V and the graduate research assistantship for M. H.. The authors acknowledge Dr. Paul King, Dr. Gordana Dukovic, and Dr. Bryant Chica for helpful discussions. The authors thank Dr. Yi Rao, Rao group members, and Buckley E. Banham for their help.

### Notes and references

- J. G. Chen, R. M. Crooks, L. C. Seefeldt, K. L. Bren, R. M. Bullock, M. Y. Darensbourg, P. L. Holland, B. Hoffman, M. J. Janik, A. K. Jones, M. G. Kanatzidis, P. King, K. M. Lancaster, S. V. Lymar, P. Pfromm, W. F. Schneider and R. R. Schrock, *Science*, 2018, **360**, eaar6611.
- L. Wang, M. Xia, H. Wang, K. Huang, C. Qian, C. T. Maravelias and G. A. Ozin, *Joule*, 2018, **2**, 1055–1074.
- G. Qing, R. Ghazfar, S. T. Jackowski, F. Habibzadeh, M. M. Ashtiani, C.-P. Chen, M. R. Smith and T. W. Hamann, *Chem. Rev.*, 2020, **120**, 5437–5516.
- C. J. M. van der Ham, M. T. M. Koper and D. G. H. Hetterscheid, *Chem. Soc. Rev.*, 2014, **43**, 5183–5191.
- A. R. Singh, B. A. Rohr, J. A. Schwalbe, M. Cargnello, K. Chan, T. F. Jaramillo, I. Chorkendorff and J. K. Nørskov, *ACS Catal.*, 2017, **7**, 706–709.
- M. J. Chalkley, M. W. Drover and J. C. Peters, *Chem. Rev.*, 2020, **120**, 5582–5636.
- D. Singh, W. R. Buratto, J. F. Torres and L. J. Murray, *Chem. Rev.*, 2020, **120**, 5517–5581.
- X. Cui, C. Tang and Q. Zhang, *Adv. Energy Mater.*, 2018, **8**, 1800369.
- A. J. Medford and M. C. Hatzell, *ACS Catal.*, 2017, **7**, 2624–2643.
- B. M. Comer, P. Fuentes, C. O. Dimkpa, Y.-H. Liu, C. A. Fernandez, P. Arora, M. Realff, U. Singh, M. C. Hatzell and A. J. Medford, *Joule*, 2019, **3**, 1578–1605.
- O. Elishav, B. Mosevitzky Lis, E. M. Miller, D. J. Arent, A. Valera-Medina, A. Grinberg Dana, G. E. Shter and G. S. Grader, *Chem. Rev.*, 2020, **120**, 5352–5436.
- P. L. Dunn, B. J. Cook, S. I. Johnson, A. M. Appel and R. M. Bullock, *J. Am. Chem. Soc.*, 2020, **142**, 17845–17858.
- F. Schüth, R. Palkovits, R. Schlögl and D. S. Su, *Energy Environ. Sci.*, 2012, **5**, 6278–6289.
- W. W. Yu and X. Peng, *Angew. Chem. Int. Ed.*, 2002, **41**, 2368–2371.
- H. Lu, Z. Huang, M. S. Martinez, J. C. Johnson, J. M. Luther and M. C. Beard, *Energy Environ. Sci.*, 2020, **13**, 1347–1376.
- S. H. Lee, D. S. Choi, S. K. Kuk and C. B. Park, *Angew. Chem. Int. Ed.*, 2018, **57**, 7958–7985.
- K. Holá, M. V. Pavliuk, B. Németh, P. Huang, L. Zdražil, H. Land, G. Berggren and H. Tian, *ACS Catal.*, 2020, **10**, 9943–9952.
- C. A. Caputo, M. A. Gross, V. W. Lau, C. Cavazza, B. V. Lotsch and E. Reisner, *Angew. Chem. Int. Ed.*, 2014, **53**, 11538–11542.
- B. L. Greene, C. A. Joseph, M. J. Maroney and R. B. Dyer, *J. Am. Chem. Soc.*, 2012, **134**, 11108–11111.
- K. A. Brown, M. B. Wilker, M. Boehm, G. Dukovic and P. W. King, *J. Am. Chem. Soc.*, 2012, **134**, 5627–5636.
- C. Hamon, A. Ciaccafava, P. Infossi, R. Puppo, P. Even-Hernandez, E. Lojou and V. Marchi, *Chem. Commun.*, 2014, **50**, 4989–4992.
- G. A. M. Hutton, B. Reuillard, B. C. M. Martindale, C. A. Caputo, C. W. J. Lockwood, J. N. Butt and E. Reisner, *J. Am. Chem. Soc.*, 2016, **138**, 16722–16730.
- Y. S. Chaudhary, T. W. Woolerton, C. S. Allen, J. H. Warner, E. Pierce, S. W. Ragsdale and F. A. Armstrong, *Chem. Commun.*, 2011, **48**, 58–60.
- X.-B. Li, C.-H. Tung and L.-Z. Wu, *Angew. Chem. Int. Ed.*, 2019, **58**, 10804–10811.
- B. Chica, C.-H. Wu, Y. Liu, M. W. W. Adams, T. Lian and R. B. Dyer, *Energy Environ. Sci.*, 2017, **10**, 2245–2255.
- M. L. K. Sanchez, C.-H. Wu, M. W. W. Adams and R. B. Dyer, *Chem. Commun.*, 2019, **55**, 5579–5582.
- M. L. K. Sanchez, S. E. Konecny, S. M. Narehood, E. J. Reijerse, W. Lubitz, J. A. Birrell and R. B. Dyer, *J. Phys. Chem. B*, 2020, **124**, 8750–8760.
- F. Kurayama, T. Matsuyama and H. Yamamoto, *Adv. Powder Technol.*, 2004, **15**, 51–61.
- F. A. Tezcan, J. T. Kaiser, D. Mustafi, M. Y. Walton, J. B. Howard and D. C. Rees, *Science*, 2005, **309**, 1377–1380.
- S. B. Jang, L. C. Seefeldt and J. W. Peters, *Biochemistry*, 2000, **39**, 14745–14752.
- O. Einsle, F. A. Tezcan, S. L. A. Andrade, B. Schmid, M. Yoshida, J. B. Howard and D. C. Rees, *Science*, 2002, **297**, 1696–1700.
- T. Spatzal, M. Aksoyoglu, L. Zhang, S. L. A. Andrade, E. Schleicher, S. Weber, D. C. Rees and O. Einsle, *Science*, 2011, **334**, 940–940.
- Z.-Y. Yang, R. Ledbetter, S. Shaw, N. Pence, M. Tokmina-Lukaszewska, B. Eilers, Q. Guo, N. Pokhrel, V. L. Cash, D. R. Dean, E. Antony, B. Bothner, J. W. Peters and L. C. Seefeldt, *Biochemistry*, 2016, **55**, 3625–3635.
- N. Pence, M. Tokmina-Lukaszewska, Z.-Y. Yang, R. N. Ledbetter, L. C. Seefeldt, B. Bothner and J. W. Peters, *J. Biol. Chem.*, 2017, **292**, 15661–15669.
- A. J. D'Eustachio and R. W. F. Hardy, *Biochem. Biophys. Res. Commun.*, 1964, **15**, 319–323.
- D. A. Ware, *Biochem. J.*, 1972, **130**, 301–302.
- A. Badalyan, Z.-Y. Yang and L. C. Seefeldt, *ACS Catal.*, 2019, **9**, 1366–1372.
- A. Badalyan, Z.-Y. Yang, B. Hu, J. Luo, M. Hu, T. L. Liu and L. C. Seefeldt, *Biochemistry*, 2019, **58**, 4590–4595.
- L. C. Seefeldt, B. M. Hoffman, J. W. Peters, S. Rauegi, D. N. Beratan, E. Antony and D. R. Dean, *Acc. Chem. Res.*, 2018, **51**, 2179–2186.
- D. Lukoyanov, N. Khadka, Z.-Y. Yang, D. R. Dean, L. C. Seefeldt and B. M. Hoffman, *J. Am. Chem. Soc.*, 2016, **138**, 10674–10683.
- M. Rohde, D. Sippel, C. Trncik, S. L. A. Andrade and O. Einsle, *Biochemistry*, 2018, **57**, 5497–5504.
- F. B. Simpson and R. H. Burris, *Science*, 1984, **224**, 1095–1097.
- W. W. Yu, L. Qu, W. Guo and X. Peng, *Chem. Mater.*, 2003, **15**, 2854–2860.
- L. C. P. Gonçalves, H. R. Mansouri, S. PourMehdi, M. Abdallah, B. S. Fadiga, E. L. Bastos, J. Sá, M. D. Mihovilovic and F. Rudroff, *Catal. Sci. Technol.*, 2019, **9**, 2682–2688.
- W. N. Lanzilotta, M. J. Ryle and L. C. Seefeldt, *Biochemistry*, 1995, **34**, 10713–10723.
- A. Braaksma, H. Haaker, H. J. Grande and C. Veeger, *Eur. J. Biochem.*, 1982, **121**, 483–491.

## ARTICLE

Journal Name

- 47 S. Y. Druzhinin, L. A. Syrtsova, A. M. Uzenskaja, G. I. Likhtenstein. *Biochemical Journal*, 1993, **290**, 627–631.
- 48 M. M. Meirovich, O. Bachar and O. Yehezkeli, *Catalysts*, 2020, **10**, 979–990.
- 49 K. A. Brown, D. F. Harris, M. B. Wilker, A. Rasmussen, N. Khadka, H. Hamby, S. Keable, G. Dukovic, J. W. Peters, L. C. Seefeldt and P. W. King, *Science*, 2016, **352**, 448–450.
- 50 K. A. Brown, J. Ruzicka, H. Kallas, B. Chica, D. W. Mulder, J. W. Peters, L. C. Seefeldt, G. Dukovic and P. W. King, *ACS Catal.*, 2020, **10**, 11147–11152.
- 51 J. Christiansen, P. J. Goodwin, W. N. Lanzilotta, L. C. Seefeldt and D. R. Dean, *Biochemistry*, 1998, **37**, 12611–12623.
- 52 C. DeBruler, B. Hu, J. Moss, J. Luo and T. L. Liu, *ACS Energy Lett.*, 2018, **3**, 663–668.
- 53 B. M. Barney, R. Y. Igarashi, P. C. Dos Santos, D. R. Dean and L. C. Seefeldt, *J. Biol. Chem.*, 2004, **279**, 53621–53624.
- 54 J. L. Corbin, *Appl. Environ. Microbiol.*, 1984, **47**, 1027–1030.